# CHAPTER-6

## Fabrication, optimization and evaluation of microspheres loaded in-situ gel (MLIG) Implants

*CHAPTER 6*

# Fabrication, Optimization and Evaluation of Microspheres Loaded In-Situ Gel (MLIG) Implants

## 6.1. METHODS

### 6.1.1. Experimental Design

A response surface methodology, 3 level, 3 factor BBED was employed to statistically optimize the processing factors of optimized microspheres loaded *in-situ* gel (MLIG) using Design-Expert software® (8.0.6.1, Stat-Ease Inc., US). Concentration of Pluronic® F127 (CP127), Pluronic® F68 (CP68) and concentration of microspheres (COM) were selected as fabrication variables for optimizing gelation temperature ($G_{temp}$) and viscosity as dependent response variables (Table 6.1).

**Table 6.1: Box-Behnken Experimental Design for the formulation of MLIG.**

| Fabrication variables | Low (-) level | Medium (0) level | High (+) level |
|---|---|---|---|
| A: Concentration of P127 (CP127) (% w/v) | 15 | 17.5 | 20 |
| B: Concentration of P68 (CP68) (% w/v) | 2 | 3 | 4 |
| C: Concentration of microspheres (COM) (% w/v) | 20 | 40 | 60 |
| **Dependent response variables** | **Constraints** | | |
| Gelation temperature ($G_{temp}$) (°C) | 34-37 °C | | |
| Viscosity (cps) | < 1000 | | |

BBED was specifically selected for its requirements of minimal experimental runs for three factors (-, 0, +). A total of 17 experimental runs were performed to estimate the full model. Polynomial equations, ANOVA results and determination of optimum values of dependent variables was done as discussed in *section 5.1.3.2.1 (Chapter 5)*.

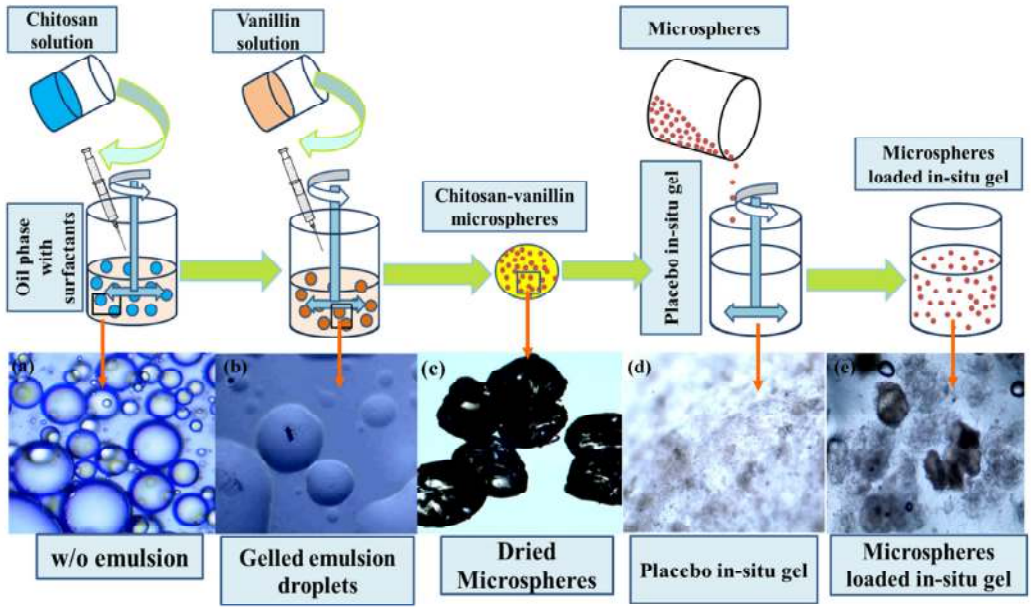


**Figure 6.1: Diagrammatic and optical microscopic illustration (a, b, c, d and e) of steps involved in the formation of crosslinked microspheres loaded *in-situ* gels (MLIG).**

### 6.1.2. Formulation of Microsphere loaded *in-situ* gel

Thermosensitive, biodegradable, mucoadhesive MLIG implants of Pluronics 127/68 were formulated by modification of cold method (Schmolka, 1972). In brief, carbopol solution (0.01%, for mucoadhesion property) was prepared in Millipore water under agitation on a magnetic stirrer and refrigerated. Further, weighed amounts of P127 and P68 were dissolved in cold (4 °C) carbopol solution under mild agitation of 50 rpm (Table 6.1). The formed solution was kept in a refrigerator for around 24 h to ensure complete dissolution of pluronics. The optimized microspheres were dispersed in

prepared aqueous Pluronic® solution under mild agitation for 15 minutes and refrigerated (Fig 6.1). Placebo gels were prepared without the microspheres. Formulations were sterilized using autoclave at 121 °C and 15 psi for 15 min.

### 6.1.3. Dependent response variables for MLIG formulations

#### 6.1.3.1. *Gelation temperature*

The $G_{temp}$ was determined using the test-tube inversion method (Baloğlu *et al.,* 2010). 2 ml of the cold *in-situ* gel was placed in a test tube, which was then immersed in a beaker containing water maintained at 15 $^{o}$C kept on a temperature regulated magnetic stirrer. The temperature of the water bath was then gradually increased, samples were examined for every two minutes and $G_{temp}$ was recorded when the gel stops flowing upon inversion of test-tube at an angle of 90 degrees.

#### 6.1.3.2. *Viscosity*

The viscosities of gels were recorded to evaluate ease of administration of formulation. The viscosity of the optimized MLIG was determined using a Brookfield DV-III Ultra programmable Rheometer (Brookfield Engineering Laboratories Inc., USA) with spindle 64 at 100 rpm after 15 sec equilibration time at room temperature.

### 6.1.4. Evaluation of optimized microspheres and MLIG

#### 6.1.4.1. *In-vitro* drug dissolution study and release kinetics

For release studies, 2 ml of cold MLIG was filled in dialysis membranes hermetically sealed at both ends and placed in 200 ml of PBS pH 6.8 contained in a beaker kept on magnetic stirrer with 100 rpm stirring maintained at 37±0.5 °C. At pre-specified time intervals (0, 0.5, 1, 2, 3, 4, 5, 6, 7, 8, 10, 12 days) the samples were withdrawn and replenished with equivalent buffer to maintain sink condition. The amount drug released was estimated using UV method as discussed in *sub-section 4.1.2.2.1*

*(Chapter 4).* Drug release kinetics was determined using various kinetic models. From Korsmeyer-Peppas equation the drug release mechanism from *in-situ* gels were estimated using release coefficient (n) values. Values of $n = 0.5$ indicates Fickian diffusion mechanism; $0.5 < n < 1$, indicates anomalous or non-Fickian release; $n = 1$ indicates zero-order release (Peppas and Khare, 1993).

### 6.1.4.2. Solid state characterisation

#### *6.1.4.2.1. Microscopic studies*

The SEM images of microspheres and *in-situ* gel were recorded as discussed in *sub-section 5.1.1.4.3.1.*

#### *6.1.4.2.2. Fourier-Transform Infrared spectroscopy*

Chemical interactions and compatibility between excipients were analyzed by FTIR spectroscopy as discussed in *sub-section 5.1.1.4.3.2.*

#### *6.1.4.2.3. Differential Scanning Calorimetry*

DSC of samples was studied by as discussed in *sub-section 5.1.1.4.3.3.*

#### *6.1.4.2.4. X-ray Diffraction patterns*

XRD patterns of samples were recorded as discussed in *sub-section 5.1.1.4.3.4.*

### 6.1.4.3. *Rheology*

The rheological behaviour of gels was evaluated by measuring viscosities at different shear rates of 0.5 to 100 rpm as discussed in *Sub-section 6.1.3.2.* The shear rate and viscosity (η) in centipoises (cps) were determined from the instrument readings and fitted to the following power law constitutive equation with flow parameters as consistency index (m) and the flow index (n) (Zaki *et al.,* 2007);

$$\eta = m\gamma^{n-1}$$

where, $n = 1$ indicates Newtonian behavior while $n < 1$, corresponds to shear thinning flow. The lower the value of (n) the more shear thinning the formulation.

#### 6.1.4.4. pH

The pH of optimized MLIG were noted at room temperature by dipping the glass microelectrode of the Deluxe pH meter (Perfit, India) into gel contained in test-tubes for 5 minutes (Govender *et al.,* 2005).

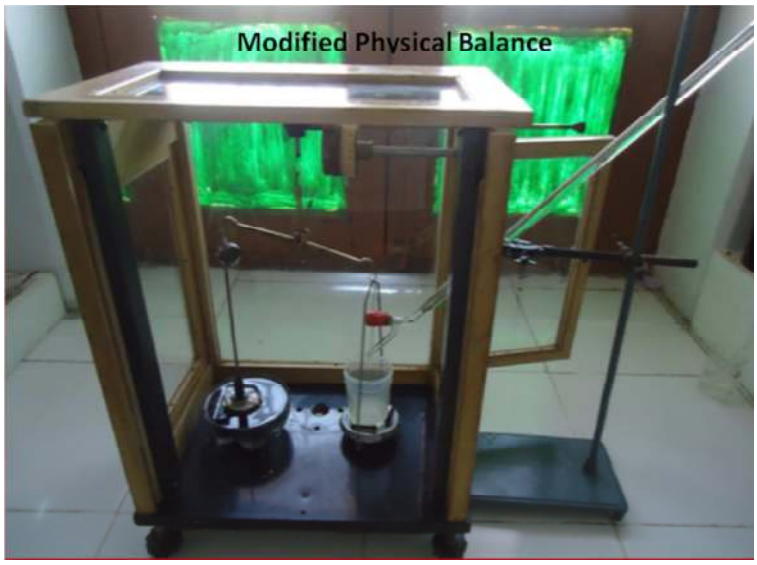


**Fig 6.2: Laboratory setup of modified physical balance for mucoadhesion studies**

#### 6.1.4.5. Mucoadhesive strength

Mucoadhesive strength of the prepared formulations was determined by the modified physical balance method (Jha *et al.,* 2011) (Fig. 6.2). The apparatus was comprised of two balance arm. On the one arm, two glass plates were attached: one was fixed to the base of the apparatus and the other one was fixed to the arm of the balance. The second arm contained the beaker. Fresh, washed bovine cheek pouch ($1x1cm^2$) was sticked to the upper and lower glass plate facing each other with the help of cynoacrylate

adhesive. About 0.5ml of formulation was placed over the tissue as a thin film on the lower plate. After that the upper plate was brought down on the lower plate and the contact pressure (preload force) of 0.2 N for 2 min was applied over the upper plate. The water was dropped from fixed height into the beaker of the second arm of balance at a rate of 2ml/minute from burette until the upper and lower plate gets detached. The weight of the water dropped into the container till detachment of plates was noted. (Patel *et al.,* 2007). The weight of water required to detach disc from the mucosal surface provided the mucoadhesive strength (N). Bond strength ($N/cm^2$), was determined from mucoadhesive strength.

$$Bond\ strength\ (\frac{N}{cm^2}) = \frac{Mucoadhesive\ strength}{tissue\ surface\ area} \times 100$$

### 6.1.4.6. Stability studies

The effect of storage on optimized batch was performed after storing samples contained in clear well closed amber glass bottles in a refrigerator for six months as on the basis of previous studies it was observed that the microspheres were stable for prolonged period at refrigerated condition. At predetermined time intervals, samples were evaluated for any change in the drug content, *in-vitro* drug release, viscosity, and $G_{temp}$. The *in-vitro* release profiles of both drugs after and before storage were compared using similarity (SF) and dissimilarity factors (DF) (Costa and Lobo, 2001). Autoclaving stability was estimated after one-time sterilization. Shelf-life of final product was determined using Minitab® 17.

### 6.1.4.7. Antimicrobial Study

The antimicrobial activity of microspheres was calculated by using drug released samples collected at 1 day and after 12 days of release studies, placebo gel and MLIG was evaluated on facultative anaerobic bacteria *viz. Staphylococcus aureus* (MTCC96; gram-positive), *Escherichia coli* (MTCC723; gram-negative) and *Enterococcus faecalis* (MTCC439; gram-positive) by disc-diffusion method as discussed in *sub-section*

*5.1.1.4.8*. Samples containing 10% DX and 25% OZ were used as the positive control for antibacterial tests.

### 6.1.4.8. Preclinical evaluation

Adult albino rats of Charles Foster strain (200±10g), of either sex were procured from the Central Animal House of the Institute of Medical Science, Banaras Hindu University. The animal study protocol was approved by Central Animal Ethical Committee (CAEC) of the Banaras Hindu University, Varanasi (no. Dean/12-13/CAEC/222) *(Annexure 1)* and carried out as per the guidelines provided by Committee for the Purpose of Control and Supervision of Experiments on Animal, Ministry of Social Justice and Empowerment, Government of India, New Delhi. The animals were accommodated in polypropylene cages with six animals per cage having free access to standard laboratory diet (Lipton feed, Mumbai, India) with water *ad libitum* kept under standard laboratory conditions of 25 °C and 55±5%.

#### *6.1.4.8.1. In-vivo biocompatibility study*

The *in-vivo* biocompatibility and degradability of freshly formulated optimized MLIG were examined by subcutaneous injections to albino rats (Chenite *et al.,* 2000). In brief, rats were shaved on the dorsal part and 0.2 ml of cold, sterilized MLIG was injected through a hypodermic syringe equipped with a 22G needle (selected based on syringeability of formulations). The animals were sacrificed by cervical dislocation after 1 day, 1, 2, 3 and 4 weeks and their surrounding tissues around injection site were retrieved postoperatively. The tissue samples were observed using optical microscope for histological parameters after staining with hematoxylin and eosin (Mi *et al.,* 2002). The control group animals were given only saline.

#### *6.1.4.8.2. In-vivo gingival tissue regeneration studies*

Ligature-Induced Periodontal (LIP) rat model was used to evaluate *in-vivo* gingival tissue regeneration ability of the developed MLIG formulations (Khan *et al.,* 2016a).

Periodontitis was induced by tying non-absorbable ligature (ETHILON, Johnson & Johnson Ltd.) around the upper incisor teeth of anesthetized rats. This induces plaque accumulation around tooth. The rats were treated into 3 groups (n = 6) as Group A (No treatment), Group B (LIP + No treatment) and Group C (LIP + MLIG) (Table 6.2).

**Table 6.2: Preclinical treatment groups and evaluation parameters for ligature induced periodontal (LIP) model.**

| Group | Treatment |
|---|---|
| A: (Control) Healthy rat | No treatment |
| B: Periodontal rat | LIP + no treatment |
| C: Treated gum | LIP + MLIG |

**Scoring evaluations**

| Scores | Tooth mobility | Gingival index | Continuity of epithelium | Continuity of transseptal fibers |
|---|---|---|---|---|
| **0** | No mobility | Normal gingival | Epithelium present along the whole interdental papilla | Intact transseptal fibers |
| **1** | Slight mobility (vestibular-palatal) | Mild inflammation, slight change in colour, edema, and no bleeding on probing | Partly absent epithelium | Partly absent transseptal fibers |
| **2** | Moderate mobility (vestibular-palatal and mesial-distal) | Moderate inflammation, redness, edema, glazing, and bleeding on probing | Completely Absence of epithelium and exudates of inflammatory cells | Absent transseptal fiber system |
| **3** | Severe mobility (vertical; the tooth moves in and out of the socket) | Severe inflammation. Redness, edema, ulceration and spontaneous bleeding | Absence of epithelium but exudate present | |

Treatment was begun on the second day after ligature application and continued for two weeks (once a week). The teeth were dissected after sacrificing rats by cervical dislocation and fixed in formalin (10% v/v), decalcified using 10% ethylene diamine tetra-acetic acid and embedded in paraffin. Serial parasagittal sections (7 mm) were cut from paraffin embedded tissue blocks. The hematoxylin and eosin stained sections were observed under optical microscope after mounting on microscope slides for changes in tissue structure. Furthermore, scoring of tooth mobility, gingival index (Xu and Wei, 2006), continuity of epithelium and transseptal fibers were performed (Table 6.2) (Khan *et al.,* 2016a).

### 6.1.4.9. Clinical Evaluation

The single blind split-mouth clinical study of optimized *in-situ* forming gels was performed after approval from Ethical Committee, Institute of Medical Sciences, BHU, India (Dean/2014-15/EC/1309) *(Annexure 2)*. Ten patients (20 - 50 years) of either sex were taken and screened based on inclusion and exclusion criteria as follows;

*Inclusion Criteria;*

1) Patients with good general health

2) Age between 20-50 years (either sex)

3) Bleeding on probing (BoP) from base of pocket

4) Patients suffering from moderate to severe periodontitis having at least three sites with pocket depth $\geq$ 5 mm

5) No periodontal therapy in last 6 months

6) No antibiotic therapy in last 1 month.

*Exclusion Criteria;*

1) Poor oral hygiene maintenance

2) Allergic history to any drug

3) Habits like smoking and pan chewing

4) Pregnant or lactating women

5) Non-availability of subjects

6) Acute oral disease

Furthermore, patients were instructed for maintenance of oral hygiene. The 3 sites in one patient were allotted to three groups as; group I (only SRP), group II (SRP + Placebo gel), and group III (SRP + MLIG), and evaluated for plaque Index (PI), gingival Index (GI), BoP, probing pocket depth (PPD) and clinical attachment level (CAL) (Khan *et al.,* 2017) (Table 6.3).

**Table 6.3: Semi-quantitative scoring of clinical parameters.**

| **Scoring of clinical parameters** | | |
|---|---|---|
| **Plaque Index** | **Gingival Index** | **Bleeding on probing (BoP)** |
| **0**-Plaque is absent in the gingival area | **0**-Normal gingival | |
| **1**-A film of plaque is present in the gingival and tooth area | **1**-Mild inflammation, slight change in color and edema with no BoP. | |
| **2**-Moderate plaque of soft tissue deposits present within gingival pocket and on the gingival margin that is visible to naked eye. | **2**-Moderate inflammation, redness, edema and glazing with BoP. | **0**- no BoP<br>**1**- BoP |
| **3**-Abundant plaque as soft tissue deposits present within gingival pocket and/or on tooth and gingival margin. | **3**-Severe inflammation, marked redness and edema, ulcerations with spontaneous BoP. | |

PI, GI and BoP were recorded at baseline before treatment, 15 days, 30 days and 60 days after treatment. PPD and CAL were reported from baseline before treatment, 30 days and 60 days after treatment. Periodontal probe (UNC 15) was used for measuring PPD and CAL.

#### 6.1.4.10. Statistical analysis

All physicochemical determinations were carried out in triplicate and results reported as mean±SD. The results of preclinical and clinical study were expressed as the mean±SEM. Statistical group comparisons of results were performed by two-way ANOVA followed by Bonferroni post-tests at 95% confidence interval using GraphPad Prism software, US.

## 6.2. RESULTS AND DISCUSSION

### 6.2.1. Formulation of *in-situ* gel

Optimized microspheres were successfully incorporated into *in-situ* Pluronic® gels. The difference in transparency of pure Pluronic® gel and MLIG are depicted in Fig. 6.3. Pluronic® are Triblock copolymers of polyethylene glycol-b-polypropylene glycol-b-polyethyleneglycol which are known to undergo temperature induced sol-gel conversion (Akash and Rehman, 2015). On increasing temperature, partial dehydration of macromolecular structure of Pluronics® occurs due to breaking of some hydrogen bonds associated with water molecules. This leads to the formation of micellar structures with the more hydrophobic polypropylene oxide (PPO) block forming the core of micelles. Further, increase in temperature brings micelles to rearrange into a gel structure (Fig. 6.3 a). This sol-gel phase transition is a reversible process, temperature dependent and depends on chemical structure of the triblock copolymer (*i.e.* type of Pluronic® and its concentration) (Al Khateb *et al.,* 2016).

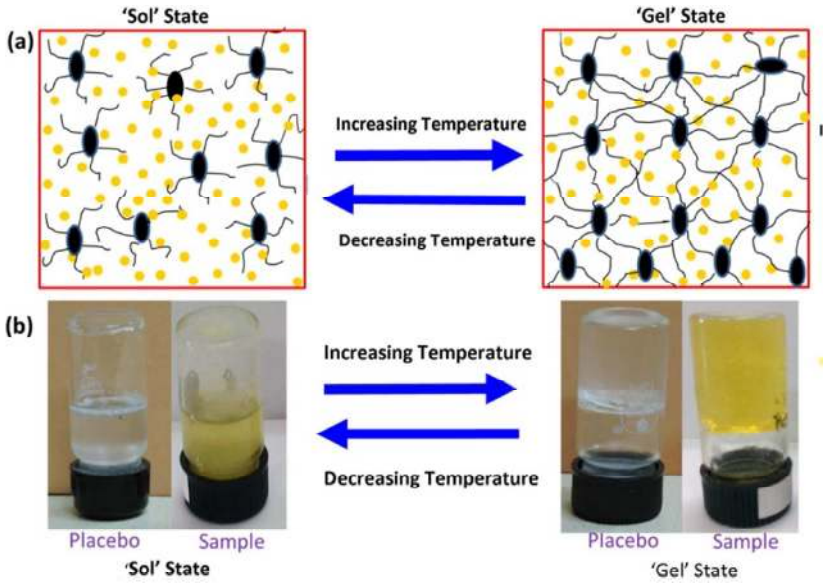


**Figure 6.3: (a) Diagrammatic and (b) Pictorial representation of mechanism 'sol' state to 'gel' state transformation of formulated thermosensitive gels.**

### 6.2.2. Dependent response variables for MLIG

#### *6.2.2.1. Gelation temperature*

$G_{temp}$ of different gel formulations varied from 29.6 to 39.6 ºC and exhibited linear relation with independent variables (Table 6.4) as put forward by following coded linear equation.

$$G_{temp} = 33.7 - 0.35*A + 3.77*B - 1.25*C - 0.15*A*B - 0.05*A*C + 0.15*B*C + 0*A^2 + 0.8*B^2 + 0.25*C^2$$

The A, B, C, and $B^2$ are significant model terms. The Model F-value of 321.46 recommended significant model (p-values < 0.050) (Table 6.5). The Lack of Fit F-value of 6.83 implied it was not significant. The Predicted $R^2$ of 0.974 was in reasonable agreement with the Adjusted $R^2$ of 0.995. Adequate Precision was greater than 4 indicated an adequate signal. Based on signs of coefficients of polynomial equations, $G_{temp}$ showed an inverse relation with P127 and concentration of microspheres (COM) and an direct relationship with concentration of P68. These results indicated increasing

P127 and COM has decreased $G_{temp}$ due to increase in solid content and more dehydration of gels. Further, increase in P68 increased $G_{temp}$ due to lack of its *in-situ* gel properties (Fig. 6.4).

**Table 6.4: Experimental runs and dependent response variables for MLIG.**

| Std run | A (P127) (w/v) | B (P68) (w/v) | C (COM) (w/v) | $G_{temp}^{*}$ (°C) (mean±SD) | Viscosity* (cps) (mean±SD) |
|---|---|---|---|---|---|
| **1** | 15 | 2 | 40 | 31.1±0.6 | 538.44±8.62 |
| **2** | 20 | 2 | 40 | 30.4±0.7 | 1112.61±9.55 |
| **3** | 15 | 4 | 40 | 38.9±1.1 | 570.25±3.71 |
| **4** | 20 | 4 | 40 | 37.6±0.9 | 1151.45±11.63 |
| **5** | 15 | 3 | 20 | 35.4±0.8 | 531.82±6.84 |
| **6** | 20 | 3 | 20 | 35.1±0.8 | 1171.42±5.65 |
| **7** | 15 | 3 | 60 | 32.9±1.3 | 573.34±6.42 |
| **8** | 20 | 3 | 60 | 32.4±1.0 | 1153.92±7.72 |
| **9** | 17.5 | 2 | 20 | 32.3±0.9 | 813.72±6.11 |
| **10** | 17.5 | 4 | 20 | 39.6±1.2 | 852.37±3.98 |
| **11** | 17.5 | 2 | 60 | 29.6±2.0 | 855.75±4.19 |
| **12** | 17.5 | 4 | 60 | 37.5±3.3 | 911.36±9.33 |
| **13** | 17.5 | 3 | 40 | 33.8±2.2 | 850.63±5.76 |
| **14** | 17.5 | 3 | 40 | 33.6±2.1 | 858.63±4.29 |
| **15** | 17.5 | 3 | 40 | 33.7±1.9 | 846.12±6.89 |
| **16** | 17.5 | 3 | 40 | 33.7±1.8 | 850.12±7.22 |
| **17** | 17.5 | 3 | 40 | 33.7±1.5 | 850.12±3.17 |

**Table 6.5. ANOVA results for MLIG**

| Response | $R^2$ | Adjusted $R^2$ | Predicted $R^2$ | Adequate Precision | F value | *p-value* Pro > F |
|---|---|---|---|---|---|---|
| **$G_{temp}$** | 0.9983 | 0.995 | 0.974 | 58.024 | 6.83 | < 0.0001 |
| **Viscosity** | 0.9959 | 0.994 | 0.991 | 75.001 | 7.97 | < 0.0001 |

### *6.2.2.2. Viscosity*

Viscosity of all batches ranged between 531. 82 to 1171.42 cps (Table 6.4). A linear relationship was exhibited between viscosity and independent variables as presented by following equation;.

$$Viscosity = +852.79+296.94*A+20.61*B+15.63*C$$

Factors A, B, and C are significant model terms. The Model F-value of 881.04 implied the model was significant (p-values < 0.050) (Table 6.5).

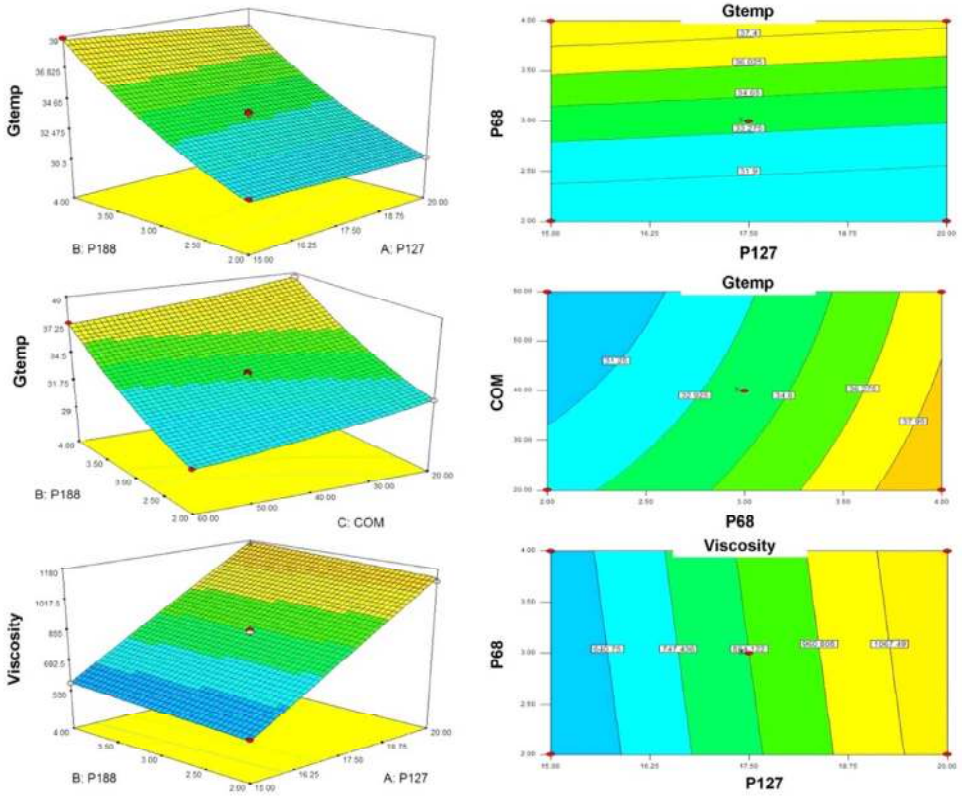


**Figure 6.4: 2D contour and 3D surface plots illustrating the effect of independent variables on responses associated with MLIG.**

The Lack of Fit F-value of 7.97 suggested the Lack of Fit was not significant and there was 11.65% chance that this could occur due to noise. Non-significant lack of fit is considered good. The Predicted $R^2$ of 0.991 was in reasonable agreement with the Adjusted $R^2$ of 0.994. Adequate Precision was greater than 4 is desirable. The positive coefficients of factors in the equation indicated that all the variables contributed towards the increasing viscosity of gel. These effects are well depicted in Fig.6.4.

### *6.2.3. Validations of model*

For validation of mathematical models, the optimized batch was formulated as P127 (15.93%), P68 (3.25%) and COM (35.38%) having $G_{temp}$ of 35.23 °C and viscosity of 663.27 cps. The % bias was calculated for each response and was found within limits (Table 6.6). The statistical analysis of results provided that the relations among variables were good fit and the model can be successfully used for predictions of results.

**Table 6.6: Validation of optimized variables for MLIG formulations**

| Variables | Optimized formulation | Desirability | | |
|---|---|---|---|---|
| A (P127) | 15.93% w/v | | | |
| B (P68) | 3.25% w/v | 1 | | |
| C (COM) | 35.38% w/v | | | |
| **Responses** | **Target** | **Predicted** | **Observed (mean±SD, n = 3)** | **% Bias** |
| **$G_{temp}$ (ºC)** | 34-37 | 34.11 | 35.23±0.21 | 3.19 |
| **Viscosity (cps)** | < 1000 | 721.33 | 663.27±5.66 | 8.75 |

### 6.2.4. Characterization of optimized microspheres and MLIG

#### 6.2.4.1. *In-vitro* drug release studies and kinetics

The *in-vitro* drug release studies of OZ and DX from optimized microspheres and MLIG implants in PBS pH 6.8 were done for twelve days and profiles are shown in Fig

6.5. Both OZ and DX are water soluble drugs and showed non-significant difference in their release profiles. The drug release profiles from microspheres and MLIG formulations are biphasic and characterized by immediate release phase followed by slow and controlled release phase. The drugs absorbed on the surface of microspheres got easily dissolved and released due to their high solubility and produced a fast release.

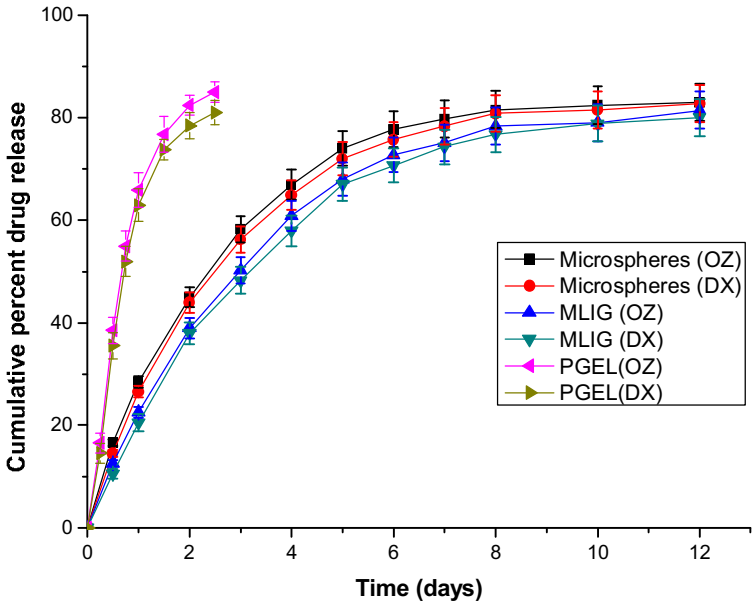


**Figure 6.5: *In-vitro* drug release studies of OZ and DX from optimized microspheres, MLIG and pluronic gels without microspheres (PGEL). Vertical bars represent SD.**

The burst release of OZ and DX from MLIG was lower than microspheres due to extra barrier networks of pluronics outside the microspheres. Anderson *et al.,* 2001, proposed that pluronics forms porous three-dimensional matrix at $G_{temp}$ which allows release of both hydrophilic and hydrophobic drugs *via.* extramicellar water channels. Moreover, the drug release from MLIG implants was slower due to the involvement of 2 steps; First step involved drug release from surface erosion or dissolution of gel. In

second step drug release occurred from microspheres. In case of Pluronic® gel (PGEL) without microsphere drug release occurred only due to first step and about 80% of drugs got released within two days.

The drug release pattern from MLIG was matrix diffusion controlled and explained by Higuchi Model ($R^2 = 0.999$) (Hu *et al.,* 2012) (Table 6.7). Further, the 'n' value was more than 0.5, indicating non-Fickian type of drug release mechanism where drug release was controlled by diffusion as well as swelling mechanism (Table 6.7). Also, high value of diffusion coefficient ($0.96 \times 10^{-5}$ $cm^2$/sec for OZ and $0.21 \times 10^{-5}$ $cm^2$/sec for DX) for both drugs proved diffusion controlled drug release from polymer matrix.

**Table 6.7: Drug release kinetics from optimized MLIG formulations.**

| Drugs | Release Kinetics | | | | | | | | | | |
|---|---|---|---|---|---|---|---|---|---|---|---|
| | **Zero-order Kinetics** | | **First-order kinetics** | | **Higuchi Kinetics** | | **Hixson-Crowell kinetics** | | **Korsmeyer-Peppas kinetics** | | |
| | K (mgh/ml) | $R^2$ | K ($h^{-1}$) | $R^2$ | K ($h^{-1/2}$) | $R^2$ | K ($h^{-1/3}$) | $R^2$ | K ($h^{-n}$) | $R^2$ | n |
| **OZ** | 12.12 | 0.851 | 2.07 | 0.923 | 40.74 | 0.999 | 0.35 | 0.998 | 0.69 | 0.998 | 0.72 |
| **DX** | 16.67 | 0.988 | 0.22 | 0.933 | 41.60 | 0.997 | 0.37 | 0.996 | 0.76 | 0.998 | 0.69 |

| **Diffusion Coefficient ($cm^2$/sec)** | |
|---|---|
| **OZ** | **DX** |
| $0.96 \times 10^{-5}$ | $0.21 \times 10^{-5}$ |

### 6.2.4.2. Solid state characterisation

#### *6.2.4.2.1. Microscopy*

Microspheres appeared almost spherical in shape (Fig 6.6 a,b and c) with some surface roughness, which might be due to the presence of free drug particles. The

microspheres were undergone through swollen (Fig 6.6 d), shrunken and degraded (Fig 6.6 f) phases during their *in-vitro* drug release period of 12 days (Fig 6.6). Microscopic studies revealed the smooth, shiny surface of placebo gel (Fig 6.6g) due to the presence of crystalline Pluronic® (Fig 6.6). The microspheres were uniformly distributed and given rough surface appearance to the MLIG within gel surface of MLIG (Fig 6.6 h and i).

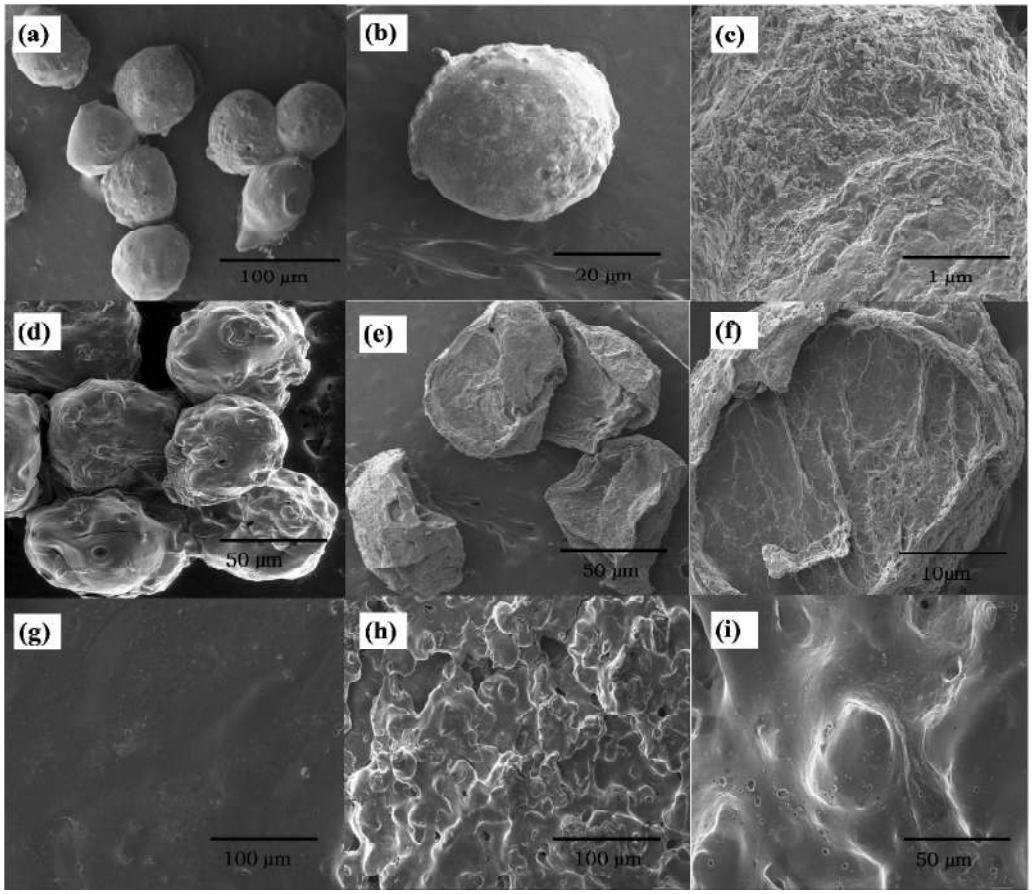


**Figure 6.6: Scanning electron microscopic view of microspheres (a-f), placebo gels (g) and microspheres loaded *in-situ* gels (MLIG) (h and i). Swollen microspheres at the end of first day of release study (d), degraded microspheres after release period of 12 days (e and f).**

### *6.2.4.2.2. Infra-red Spectroscopy*

Infrared spectra of drugs and excipients were plotted between wavenumber ($cm^{-1}$) and % transmittance (Fig 6.7). Typical absorption peaks at 2876, 3424 and 1091 $cm^{-1}$ attributed to –OH, $–NH_2$ groups and -C-O-C- linkage is recognized for polysaccharide structure of CS. The typical stretching vibrations of –OH and >C=O were observed at 3170 and 1665 $cm^{-1}$ in the spectra of VAN. The absorption bands obtained at 1590, 1510, and 815 $cm^{-1}$ belongs to benzene ring of VAN. The peculiar peak at 1266 $cm^{-1}$ belonged to the bending vibration of phenolic -OH of VAN (Fig 6.7a). Physical mixtures exhibited all the peaks of OZ, DX, CS and VAN, and indicated compatibility among the drugs and polymers.

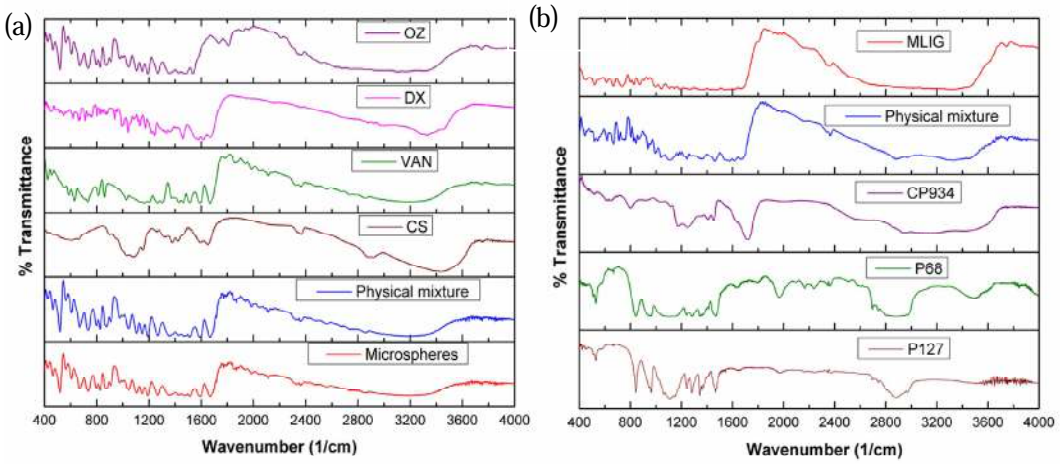


**Figure 6.7: Infrared spectra of (a) OZ, DX, VAN, CS, their physical mixture and microspheres; (b) P127, P68, CP934, their physical mixture, and MLIG**

CS-VAN microspheres showed distinguishing absorption bands at 1710 $cm^{-1}$ representing the Schiff base formation (C=N) due to interaction of aldehyde group of VAN with amino group of CS (Yang *et al.,* 2014). Moreover, the shifting of -OH peaks of CS from 3424 to 3415 $cm^{-1}$ with reduced intensity, could be attributed to H-bonding interactions between CS and VAN. These results indicated that CS could be

successfully cross-linked with VAN *via* Schiff base formation and H- bonding interactions (Zhang *et al.,* 2014).

IR spectra of Pluronic® (P127/68) was characterized by principal peaks at 3451 $cm^{-1}$, 2880 $cm^{-1}$, 1354 $cm^{-1}$, and 1106 $cm^{-1}$ owing to terminal -OH group, C-H stretching, O-H bending and C-O stretching (Fig 6.7). Infrared spectrum of carbopol 934P was characterized by principal absorption peaks at 3090 $cm^{-1}$ (O-H stretching), and 1707 $cm^{-1}$ (carboxyl group). The physical mixture and lyophilized MLIG showed all the distinct peaks for drugs and polymers indicating absence of any chemical interactions between constituents.

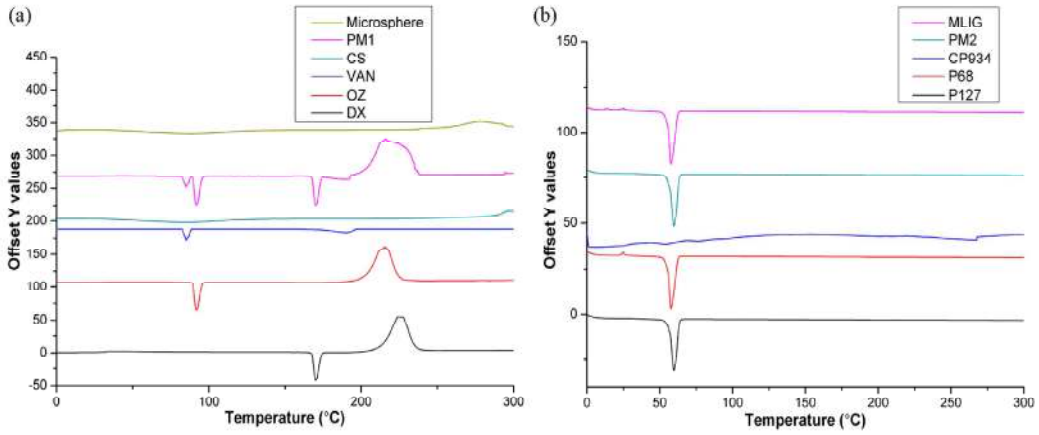


**Figure 6.8: DSC spectra of (a) DX, OZ, VAN, CS, PM1 (physical mixture of DX, OZ, VAN, CS at 1:1:1:1) and microspheres, (b) P127, P68, CP934, PM2 (physical mixture of P127, P68, CP934 and microspheres at 1:1:1:1) and MLIG.**

### *6.2.4.2.3. Differential Scanning Calorimetry*

The DSC study revealed the transition behavior of samples with increment in temperature (Fig 6.8 a and b). OZ and DX exhibited sharp melting peaks at 92 and 169 °C, respectively due to their crystalline nature (Fig 6.8). The exothermic peaks appeared above 200 °C for OZ and DX corresponded to decomposition. In addition, sharp melting

peak exhibited by VAN at 85 °C due to crystalline structure. Besides, CS, microspheres and CP934 furnished flat curves due to their amorphous nature. Amorphous character of microspheres supports the conversion of crystalline drugs and VAN into amorphous form. On the contrary, P127 and P68 showed melting point (as indicated by sharp endothermic peak) at 58.5 °C due to its crystalline state which was well preserved into MLIG thermogram (Yadav *et al.,* 2012). This may be due to higher content of Pluronic®, mild process conditions during the preparation of MLIG.

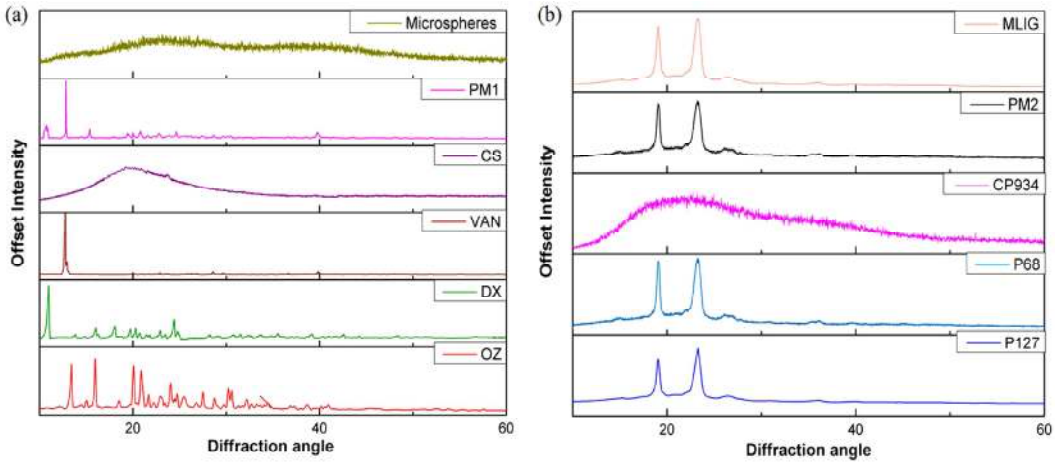


**Figure 6.9: XRD patterns of (a) OZ, DX, VAN, CS, PM1 (physical mixture of DX, OZ, VAN, CS at 1:1:1:1) and drug loaded microspheres, (b) P127, P68, CP934, PM2 (physical mixture of P127, P68, CP934 and drug loaded microspheres at 1:1:1:1) and MLIG.**

#### *6.2.4.2.4. X-Ray Diffraction*

The outcomes of DSC thermograms were further supported by XRD patterns. OZ, DX and VAN exhibited sharp diffraction peaks attributed to their crystalline state (Fig 6.9 a and b). These crystalline peaks were absent in drug loaded microspheres but present in physical mixture (PM1). Absence of crystalline peaks in formulation indicates transformation of drugs and VAN into amorphous form during formulation of microspheres. Pluronic® showed two featured peaks at 19.2° and 24° ascribed to its

crystalline structure. CS and carbopol with flat curve revealed amorphous behavior. The PM2 and MLIG showed crystalline peaks similar to Pluronic® indicating crystalline state of gel.

#### 6.2.4.3. Rheological studies

The requirement of amount of gel for introducing into the periodontal pockets is extremely low, and it is necessary to raise the viscosity for better retention in the periodontal pocket and better control of drug release. On the other hand, to instill easily in the periodontal pocket, the formulation should have an optimum viscosity. Hence, the viscosity of sols of various formulations was determined at 25 °C at 100 rpm. It is worth mentioning that the determination of viscosity at 37 °C was not feasible due to formation of stiff gel.

Fig. 6.10 shows shear rate vs. viscosity plot. Newtonian or pseudoplastic flow is desirable for the injectables as it provides less resistance during syringeability. The value of n was found 0.728 which was less than 1, thus corresponds to shear-thining system or pseudoplastic flow. The consistency index (m) was 2653.6 indicative of lower viscosity at shelf condition. This type of fluids displays a decreasing viscosity with an increasing shear rate. The changes in viscosity with rotation of spindle are attributed to temporary changes in the structure of molecules by orienting parallel to the spindle surface. At faster spindle rotation, there is more destruction of molecular structure leading to less sliding of molecules and lower viscosity. The optimized MLIG were easily syringeable with 22G syringe needles due to lower viscosity.

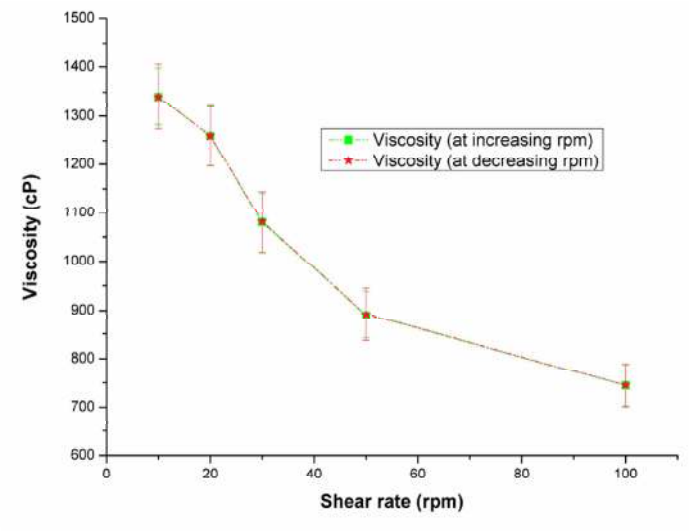


**Figure 6.10: Rheology of gels. Viscosity measurements at 25 °C.**

### *6.2.4.4.* pH

The surface pH of optimized MLIG batch was found to be 6.7±0.87 which was near neutrality and closer to the pH of GCF and acceptable for periodontal applications.

### 6.2.4.5. Swelling and erosion studies

The swelling and erosion curves of MLIG implants in simulated saliva pH 6.8 are shown in Fig. 6.11 (a and b). Maximum swelling was obtained in four days. About 20% erosion of formulations were observed in 14 days. The swelling may be attributed to increase in size of microspheres and ersoion occured by dissolution of water soluble pluronics as discussed in drug release section.

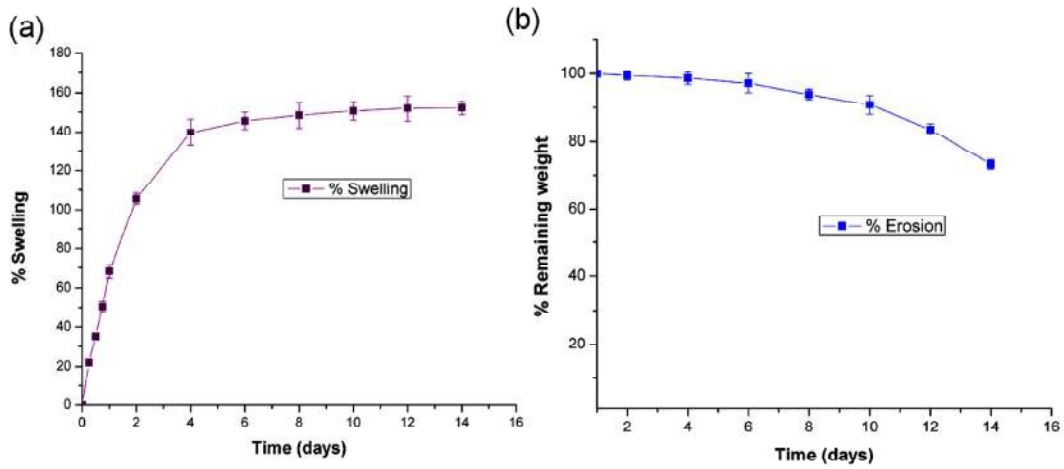


**Figure 6.11: Swelling and erosion studies of MLIG in simulated saliva pH 6.8.**

### *6.2.4.6. In-vitro Mucoadhesion*

Mucoadhesion is an important parameter for estimation of stay of microspheres at its site of action. Optimized MLIG formulations provided mucoadhesion force as 0.0086 N and bond strength of 0.0086 (N $cm^{-2}$). This result supports the possibility of retention of microspheres for extended time into periodontal pockets regardless of GCF flow. Such high mucoadhesive property of microspheres was contributed by cationic 0.01% carbopol and CS microspheres due to their cationic surface. Thus, enhancement in retention of MLIG was observed on the mucosal surfaces.

### 6.2.4.7. Stability study

Stability of optimized MLIG implants was studied after sterilization and storage in refrigerator for 6 months by evaluating changes in $G_{temp}$, viscosity, drug content and drug release. The summary of stability parameters of MLIG formulations after sterilization and storage are illustrated in Table 6.8. Results demonstrated non-significant changes in drug content, $G_{temp}$, viscosity and drug release profiles of both drugs was observed. Furthermore, SF and DF outcomes supported similarity of drug release profiles after sterilization and storage.

**Table 6.8: Stability studies of optimized MLIG formulations after sterilization and storage at refrigerated condition.**

| Parameters | | Fresh sample | After sterilization | After refrigeration |
|---|---|---|---|---|
| | **$G_{temp}$(°C)** | 35.23±0.21* | 35.27±0.43* | 35.66±0.37* |
| | **Viscosity (cps)** | 663.27±5.66* | 663.28±0.38* | 666.05±0.27* |
| **DX** | **DX content (%)** | 99.78±0.34* | 98.11±0.55* | 95.68±0.61* |
| | **TDX (days)** | 11.12±0.26* | 11.14±0.19* | 10.34±0.47* |
| | **SF (f1)** | - | 0.17# | 0.91# |
| | **DF (f2)** | - | 99.92# | 97.75# |
| **OZ** | **OZ content (%)** | 99.83±0.36* | 99.08±0.27* | 96.82±0.48* |
| | **TOZ (days)** | 10.22±0.17* | 10.19±0.43* | 9.86±0.64* |
| | **SF (f1)** | - | 0.18# | 1.18# |
| | **DF (f2)** | - | 99.89# | 96.56# |

Note: SF (f1) - similarity factor, DF (f2) - dissimilarity factor, TOZ- time for 80% cumulative OZ release; TDX - time for 80% cumulative DX release. *Values are mean±SD, n = 3. #Similarity demonstrated.

. In addition, non-significant changes in the parameters over six months of storage may be attributed to low temperature of storage and high concentration of Pluronic®. The shelf-life estimated based on the period in which the drug content reduced to 90% was estimated. As there were two drugs the shelf-life was determined by the fast degrading drug DX. The shelf life was found as 11.29 months for MLIG implants at refrigerated conditions (Fig 6.12).

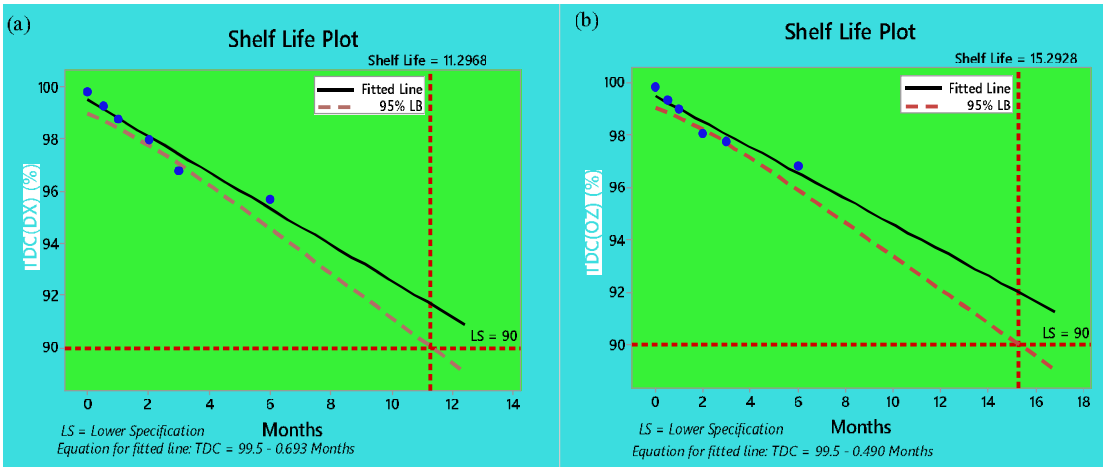


**Figure 6.12: Shelf-life plots of optimized MLIG formulations. (a) Shelf-life plot as per DX concentration. (b) Shelf-life as per OZ concentration after storage.**

### 6.2.4.8. Antimicrobial activity study

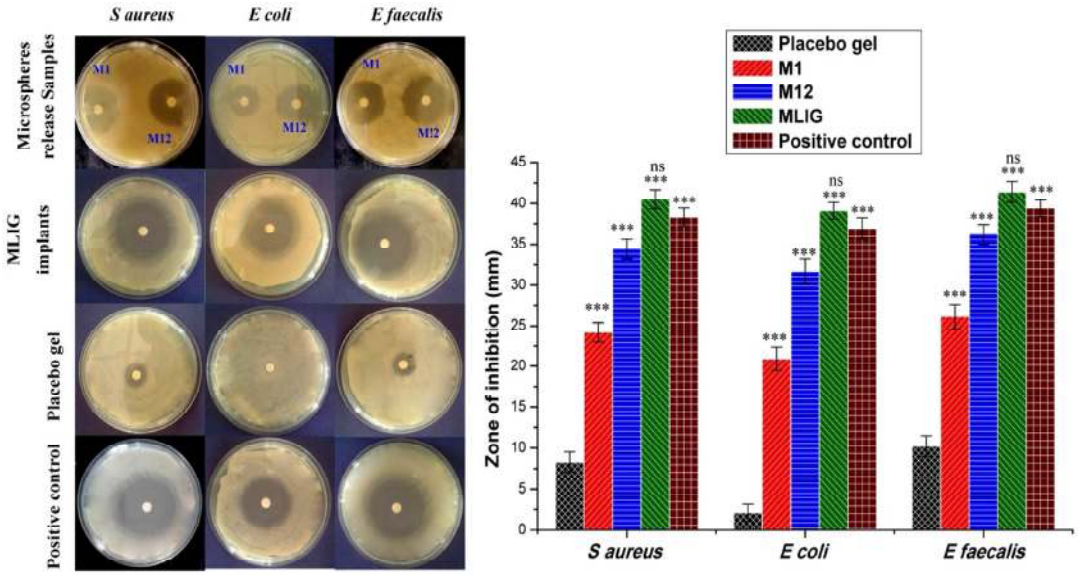


**Figure 6.13: Antimicrobial activity of microspheres (drug release samples after 1 day (M1) and 12 days (M12)), Placebo gel and MLIG formulations. Vertical bars represents SEM. $^{***}p < 0.001$ as compared to placebo gel, $^{ns}p > 0.05$ - non-significant as compared to positive control.**

The antimicrobial activity of microspheres release samples of microspheres, placebo gel and MLIG was estimated by measuring zone of inhibition against *S. aureus*, *E. coli* and *E. faecalis* (Fig. 6.13). These are common super-infecting bacteria's obtained from periodontal isolates that are responsible for endodontic treatment failures and has been reportedly used to prove the efficacy of periodontal medicines (Jain *et al.,* 2016; Khan *et al.,* 2016b; Verdugo *et al.,* 2016). In case of release samples of microspheres after one day (M1) and 12 days (M12) significant zones ($p < 0.001$) of inhibition was obtained as compared to placebo gel indicating maintenance of activity of formulations for 12 days against selected microbes.

Similarly, the antibacterial activity of MLIG implants was also supported by large and significant values of zones of inhibitions against all selected pathogens as compared to placebo gel while it was non-significantly ($p > 0.05$) different from the positive control (Fig. 6.13). Also, efficacy of formulations against microbes followed order of *E. faecalis >E. coli > S. aureus*. The antimicrobial activity of formulations corresponded to collective effect of OZ and DX antimicrobials which are active against gram-positive as well as gram-negative bacteria. Although the studies were performed on these prevalent microbes for periodontal condition, it can be very obvious that the formulations will be effective against microbes falling in the spectrum of activity of incorporated drugs. This type of combination of drugs had been reportedly found active against *Aggregatibacter actinomycetemcomitan* (Aitken *et al.,* 1992).

In addition to drug incorporated formulations, little antimicrobial activity was exhibited by placebo gels that can be attributed to presence of carbopol and Pluronic® (Dos Santos *et al.,* 2011). Thus, it can be inferred that combination of drugs has provided better activity against broad range of microbes and can be used for the treatment of periodontitis.

### 6.2.4.9. Preclinical study

#### *6.2.4.9.1. Biocompatibility studies*

The implants were injected subcutaneously into the back regions (left or right) of rats and observed for local tissue irritation reactions by optical microscope for 4 weeks (Fig 6.14). Very prompt and significant inflammatory responses were visible at first day of injection (Fig 6.14). Immediate infiltrations of inflammatory cells (macrophages, neutrophils and giant cells) can be observed. A large number of inflammatory mediators such as macrophages, neutrophils, and polymorphonuclear (PMN) cells were identified infiltrated around the implant. This is general predictable tissue response to any foreign body invasion or injury to tissue (Kang and Singh, 2005).

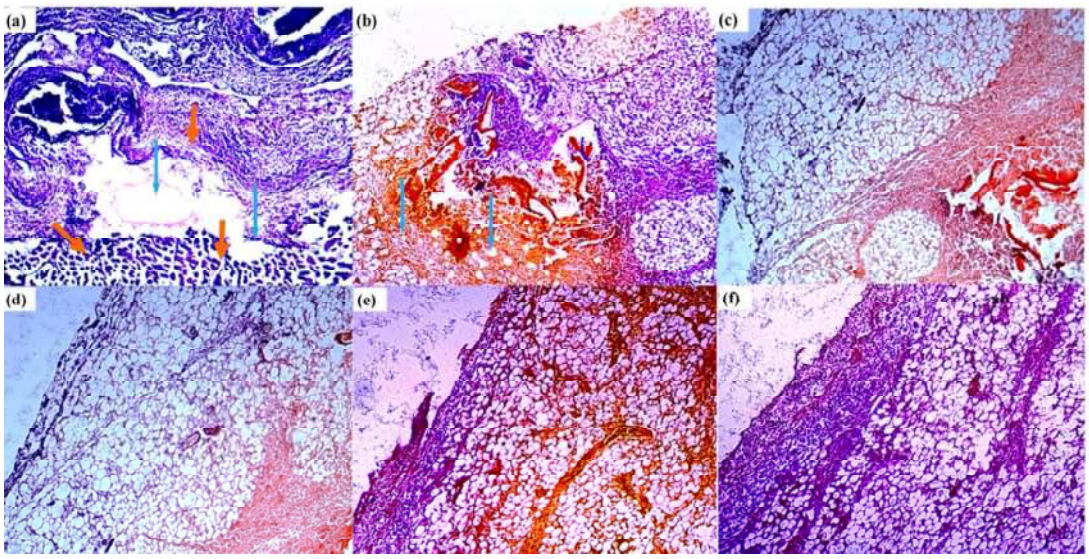


**Figure 6.14: Histopathological images of subcutaneous tissue of rats injected with MLIG at 40X magnification. (a) Non-stained MLIG formulations (green arrow) surrounded by macrophages (red arrow) at day 1. (b) 1st week (c) 2nd week (d) 3rd week (e) 4th week- inflammatory cells almost disappeared and no significant inflammatory cells were observed and (f) Control.**

At the end of 2nd and 3rd week these inflammatory mediators disappeared and normal tissue appeared (Fig 6.14c and d).After the acute inflammation phase, the cells

usually started disappearing with time. Further, the disappearance of gel and microspheres after 4 weeks may be credited to their dispersion into tissue and degradation.

Macrophages play critical role in the phagocytosis and degradation of formulations *in-vivo.* Normal tissues regenerated after 4 weeks with no evidence of any tissue damage, which was highly comparable to the control tissue sample (Fig 6.14e and f). Due to localized application of the gel, local tissue reactions are more concerned than systemic reactions. All the polymers and drugs used in this study were FDA approved and biocompatible (Maheshwari *et al.,* 2006; Yuan *et al.,* 2012). Further, no unexpected tissue reactions were observed indicating biocompatibility of gels for intrapocket use in periodontal infection.

#### *6.2.4.9.2. Tissue regeneration studies*

Graded responses for all parameters including tooth motility, gingival index, continuity of epithelium and transseptal fibers of treated rat groups (group III) showed non-significant ($p > 0.05$) change at the end of treatment period as compared to control group I (Fig 6.15a). Fig 6.15 b-g, illustrates microscopic differences in gingival tissues of control (group I), periodontal (group II) and treated rats (group III).

These results were further verified from the outcomes of microscopic studies regarding wound healing and connective tissue regeneration (Fig 6.15 b-g). Destruction of gingival tissue ligaments (lg) and inflammation was apparent as early as after the insertion of a ligature (Fig 6.15 c and f) as compared to control. Infiltration of monocyte (mc) and large, multinucleate osteoclasts (oc) cells were spotted closer to alveolar bone (ab) resorption area. Also, regeneration of damaged periodontal ligaments (lg) after one and two weeks of treatment to rats was observed. The growth and regeneration of periodontal ligaments are well distinguished after two weeks of treatment (Fig 6.15 e and g).

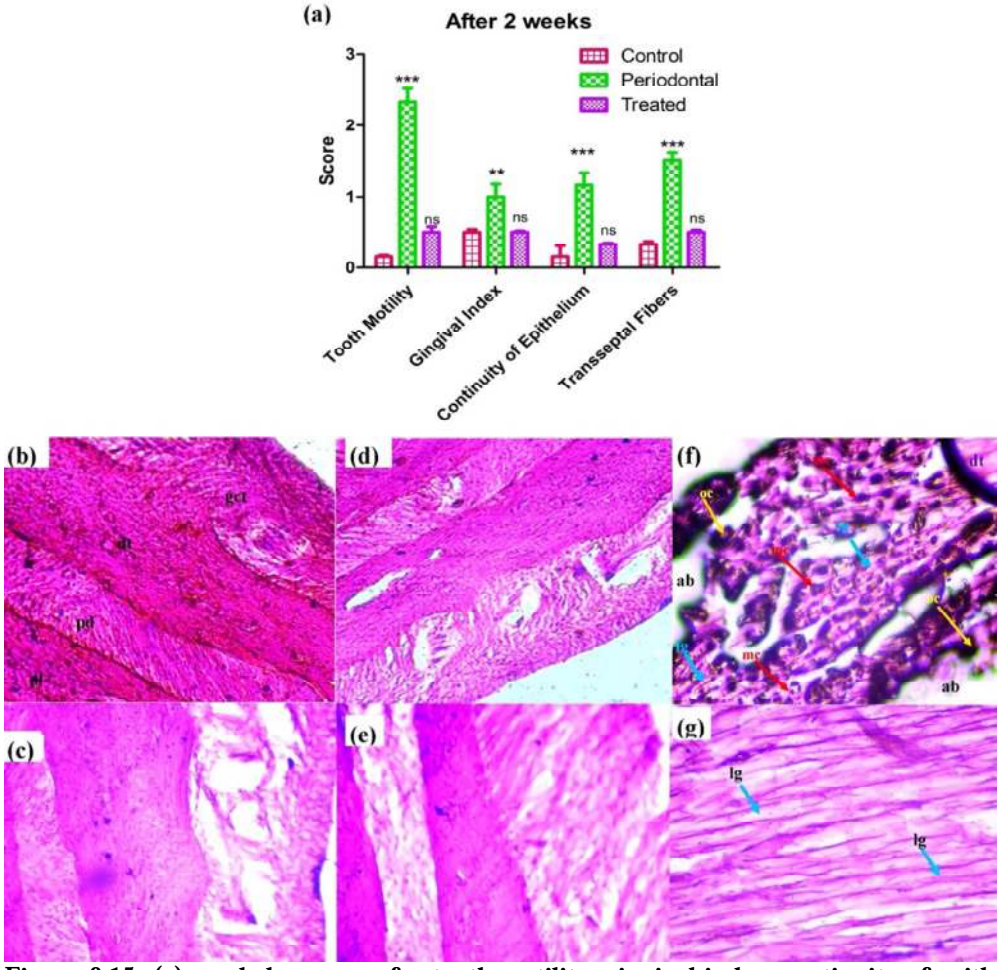


**Figure 6.15: (a) graded response for tooth motility, gingival index, continuity of epithelium and transseptal fibers were noted in group I (Control), Group II (Periodontal rats) and Group III (Treated rats) after 2 weeks. **$p < 0.01$ and ***$p < 0.001$ compared to group I (Control), ns - non-significant as compared to control by two-way ANOVA followed by Bonferroni post-tests. Vertical bars represents SEM, $n = 6$. (b, c, d and e) Microscopic observations of differentiation of gingival connective tissue (gct), dentine (dt), predentine (pd), pulp (pl) and alveolar bone (ab) of rats after LIP (10 X). (b) Group I; (c) Group II; Group III (d) After 1 week of treatment; and (e) after 2 weeks of treatment. (f and g) High magnification images (40 X), (f) showing damaged 'gct' and inflammatory response in periodontal rats. Monocyte (mc) infiltration (red arrow) and damaged periodontal ligaments (lg) (blue arrow) in the 'gct' as a result of ligature placement, the cells were stained blue containing condensed nuclei and little cytoplasm. Also, some motile, large and multinucleate osteoclasts 'oc' cells (yellow arrow) can be observed near bone resorption area *viz.* alveolar bone (ab), and (g) regenerated ligaments (lg) after 2 weeks of treatment period.**

These results can also be attributed to the combined antimicrobial activity of OZ and DX. Besides, DX at low concentrations may have reduced alveolar bone loss and promoted tissue regeneration by preventing destruction of periodontal attachment by inhibiting MMPs, collagenases and gelatinases from both infiltrating cells and resident cells of the periodontium (Ciancio and Ashley, 1998).

The physiology of periodontal tissue of rats was found very similar to that of humans. The LIP in rats has exhibited enormous similarity related to the development and execution of inflammatory responses as well as gingival regeneration and wound healing with periodontitis of humans (Jacob and Nath, 2013). Therefore, LIP rat models have been reportedly used to evaluate progression and treatment of disease. However, due to loosening of ligature the treatment period was limited for two weeks.

### 6.2.4.10. Clinical evaluations

Clinical study was conducted to assess the efficacy and therapeutic potential of MLIG implants of OZ and DX in the patients suffering from the severe chronic periodontitis. Fig 6.16 (a, b, and c) shows the photographs taken during pocket depth measurement, injection of placebo gel and MLIG. During follow up studies patients reported no complaints and no signs of inflammation, irritation and pus formation, thus supporting acceptability of gels.

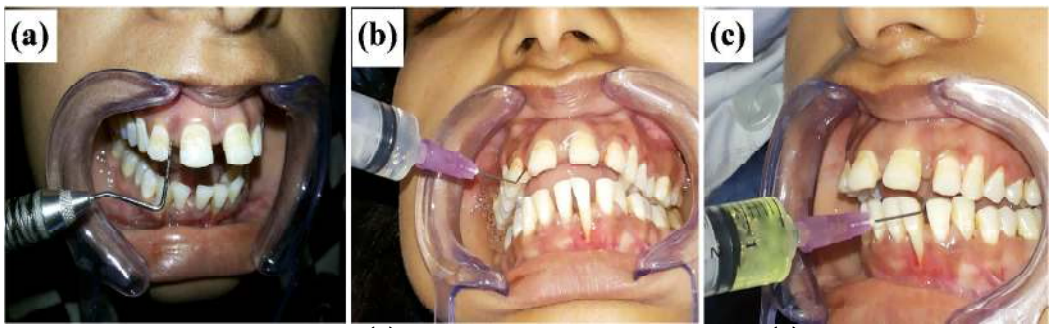


**Figure 6.16: Photographs of (a) Pocket depth measurement; (b) Injection of placebo gels; and (c) Injection of MLIG formulations.**

The results of clinical study were presented in Fig. 6.17 and 6.18, for all groups as mean reduction of the tested parameters following 60 days of treatment relative to the baseline values.

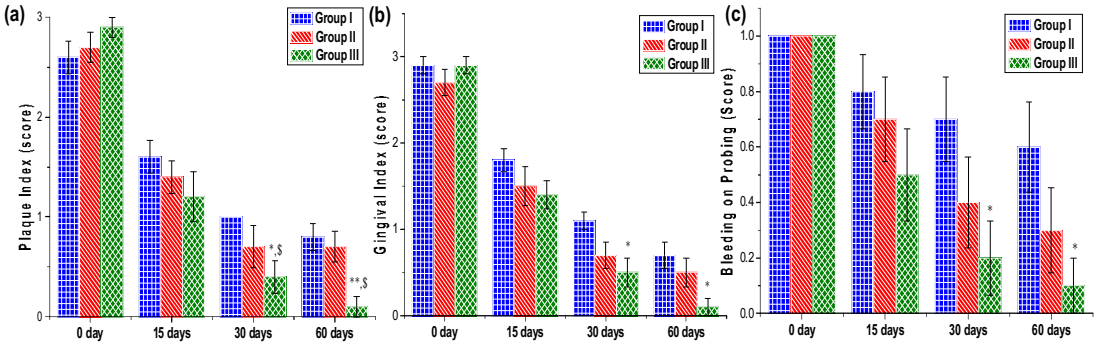


**Figure 6.17: Graphs showing changes in clinical parameters; (a) PI, (b) GI, (c) BOP. Vertical bars represent SEM, n = 10. *p < 0.05 and **p < 0.01 compared to group I, $ p < 0.05, as compared to group II by two-way ANOVA followed by Bonferroni post-tests.**

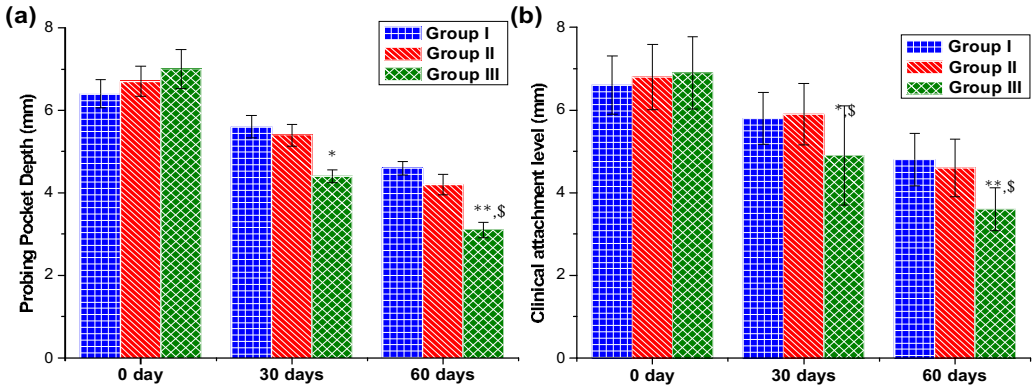


**Figure 6.18: Graphs showing measurement of clinical parameters; (a) PPD and (b) CAL. *p < 0.05 and **p < 0.01 compared to group I, $ p < 0.05 as compared to group II by two-way ANOVA followed by Bonferroni post-tests. Vertical bars represent SEM, n = 10.**

Reduction in scores of BoP, GI and PI was observed after 15 days though it was non-significant (Fig. 6.17). However, a significant reduction of clinical parameters (BoP,

GI and PI) after 30 and 60 days was evident in Group III when compared with Group I. At the end of study period, BoP ($p < 0.05$), GI ($p < 0.05$) and PI ($p < 0.01$) got significantly reduced in Group III as compared to control. Similarly, a significant reduction of PPD ($p < 0.01$) and CAL ($p < 0.01$) in group III, indicated tissue regeneration and reattachments of ligaments in comparison with Group I (Fig 6.18). Further, as compared to SRP + placebo gels (Group II), the SRP + MLIG groups (Group III) provided significant reduction ($p < 0.05$) in PI, PPD, CAL and non-significant reduction of all other parameters. These results may be attributed to little antimicrobial activity of placebo gels and confirms enhancement of therapeutic efficacy due to strong jointed antimicrobial effect of OZ and DX (Salvi *et al.,* 2002).

After the treatment of 60 days, results of clinical study revealed gels were well tolerated and gum turned into normal pink with no signs of irritation and inflammation. Although, SRP applied for the treatment of periodontal pockets is effective but group III treated with SRP along with MLIG confirmed significantly higher improvement compared to the group I and II. Further, reattachment of periodontal ligaments and significant reduction in pocket depth was seen. The split-mouth clinical treatment reduces variability in outcomes caused by risk factors (age, gender, stress, and host immune defense mechanism) related to physiology and periodontal status of patients (Khan *et al.,* 2016b).